Transcriptional Responses of *Streptococcus gordonii* and *Fusobacterium nucleatum* to Coaggregation

Naresh V.R. Mutha[1#], Waleed K. Mohammed[2,3#], Natalio Krasnogor[4], Geok Y. A. Tan[1], Siew Woh Choo[1,5,6]* and Nicholas S. Jakubovics[2]*

#Joint first author
*Joint corresponding author

1. Institute of Biological Sciences, Faculty of Science, University of Malaya, Kuala Lumpur, Malaysia. 2. School of Dental Sciences, Centre for Oral Health Research, Newcastle University, Newcastle upon Tyne, UK; 3. Department of Basic Science, College of Dentistry, University of Anbar, Ramida, Anbar, Iraq; 4. Interdisciplinary Computing and Complex Biosystems (ICOS) research group, School of Computing, Newcastle University, Newcastle upon Tyne, UK; 5. Department of Biological Sciences, Xi'an Jiaotong-Liverpool University, Suzhou Dushu Lake Science and Education Innovation District, Suzhou Industrial Park, Suzhou, P. R. China 215123; 6. Suzhou Genome Centre (SGC), Health Technologies University Research Centre (HT-URC), Xi'an Jiaotong-Liverpool University, Suzhou Dushu Lake Science and Education Innovation District, Suzhou Industrial Park, Suzhou, P. R. China 215123.

Running head: Coaggregation-mediated gene regulation

Keywords: Biofilms, Gene regulation, Molecular Oral Microbiology, Oral Microbiology Ecology, Sialic acid, *Streptococcus*

***Correspondence:**
Nicholas S. Jakubovics, Centre for Oral Health Research, School of Dental Sciences, Newcastle University, Framlington Place, Newcastle upon Tyne NE 2 4BW, UK; Tel: +191 208 6796; Fax: +191 208 8807; Email: nick.jakubovics@newcastle.ac.uk

Siew Woh Choo, Department of Biological Sciences, Xi'an Jiaotong-Liverpool University, Suzhou Dushu Lake Science and Education Innovation District, Suzhou Industrial Park, Suzhou, P. R. China 215123; Email: lawrence.choo@xjtlu.edu.cn

ABSTRACT

Cell-cell interactions between genetically distinct bacteria, known as coaggregation, are important for the formation of mixed-species biofilms such as dental plaque. Interactions lead to gene regulation in the partner organisms that may be critical for adaptation and survival in mixed-species biofilms. Here, gene regulation responses to coaggregation between *Streptococcus gordonii* and *Fusobacterium nucleatum* were studied using dual RNA-Seq. Initially, *S. gordonii* DL1 was shown to coaggregate strongly with *F. nucleatum* in buffer or human saliva. Using confocal laser scanning microscopy and transmission electron microscopy, cells of different species were shown to be evenly distributed throughout the coaggregate and were closely associated with one another. This distribution was confirmed by serial block face sectioning scanning electron microscopy, which provided high resolution 3D images of coaggregates. Cell-cell sensing responses were analysed 30 min after inducing coaggregation in human saliva. By comparison with monocultures, 16 genes were regulated following coaggregation in *F. nucleatum* whereas 119 genes were regulated in *S. gordonii*. In both species, genes involved in amino acid and carbohydrate metabolism were strongly affected by coaggregation. In particular, one 8-gene operon in *F. nucleatum* encoding sialic acid uptake and catabolism was up-regulated 2- to 5-fold following coaggregation. In *S. gordonii*, a gene cluster encoding functions for phosphotransferase system-mediated uptake of lactose and galactose was down-regulated up to 3-fold in response to coaggregation. The genes identified in this study may play key roles in the development of mixed-species communities and represent potential targets for approaches to control dental plaque accumulation.

INTRODUCTION

Oral bacteria live in structurally and functionally organized communities on the surfaces of hard and soft tissues in the mouth.[1] Biofilms on the tooth surface are particularly important since they are responsible for dental caries and periodontitis, two of the most prevalent diseases in humans worldwide.[2] These biofilms, known as dental plaque, form by the sequential colonization of bacteria present in saliva. Pioneer colonizers, including several species of oral streptococci such as *S. gordonii*, *S. sanguinis*, and *S. oralis*, along with *Neisseria*, *Haemophilus*, *Veillonella*, *Actinomyces* and others, adhere to protein and glycoprotein receptors in the acquired enamel pellicle that coats the tooth surface.[3] These species provide new adhesins and receptors that support the incorporation of other organisms into the biofilm. Genera such as *Fusobacterium* and *Corynebacterium* adhere to a large number of different oral bacteria and they can frequently be identified in the middle layers of dental plaque, potentially providing a bridge for the subsequent colonization by a diverse array of other oral bacteria.[4,5]

Many physical interactions (coaggregation) between taxonomically distinct oral bacteria have been studied *in vitro* and a number of cell surface protein adhesins and receptor carbohydrates have been identified.[6] In some cases, strong coaggregation is mediated by interactions between one type of adhesin and a complementary receptor. For example, *S. gordonii* DL1 SspB is necessary and sufficient for binding to an *Actinomyces oris* MG1 cell surface carbohydrate and mediating coaggregation.[7,8] Other coaggregation interactions involve multiple proteins and/or carbohydrates. Recent evidence indicates that coaggregation between *Fusobacterium nucleatum* and *S. gordonii* involves at least three *F. nucleatum* outer membrane proteins: two arginine-inhibitable adhesins, RadD and CmpA, and an accessory protein Aid1 that facilitates RadD-mediated adhesion.[9-12] It is not clear which components of *S. gordonii* are

45 required for this interaction, but it is likely that at least one antigen I/II family adhesin, SspA or
46 SspB, is involved since the homologous protein of *S. mutans,* SpaP, is required for coaggregation
47 with *F. nucleatum*.[13]

48 Coaggregation interactions directly influence the spatial positioning of different species
49 in dental plaque.[14] They may also play an indirect role, through bringing cells into close
50 proximity where they exchange signals, metabolites or antimicrobial products that can
51 subsequently lead to co-operative or competitive interactions in the biofilm.[15-17] Many examples
52 of metabolic cross-talk between oral bacteria have been identified.[18] Oral streptococci such as *S.*
53 *gordonii* are important producers of lactic acid that can be utilized by other species in the biofilm
54 such as *Veillonella* spp. and *Aggregatibacter actinomycetemcomitans.*[19-21] Production of 4-
55 aminobenzoate/para-amino benzoic acid (pABA) by *S. gordonii* supports biofilm formation and
56 colonization of *Porphyromonas gingivalis* in a murine oral infection model, but reduces
57 virulence.[22] *S. gordonii* also secretes ornithine during uptake of arginine through the ArcD
58 arginine/ornithine antiporter. The ornithine can be utilized by *F. nucleatum* and promotes dual-
59 species biofilm formation.[23]

60 There is now strong evidence that cell-cell interactions are sensed by the partner species
61 and lead to phenotypic adaptations that affect key functions such as growth, virulence or mixed-
62 species biofilm formation. For example, *S. gordonii* utilizes a secreted protease, Challisin, to
63 acquire and sense arginine following coaggregation with *Actinomyces oris*, and coaggregation
64 enables growth of *S. gordonii* in arginine-depleted media.[24,25] Interactions with *S. gordonii* lead
65 to up-regulation of the *A. actinomycetemcomitans* complement resistance protein ApiA and
66 promote survival in human serum.[26] In addition, in response to hydrogen peroxide production by
67 *S. gordonii*, *A. actinomycetemcomitans* up-regulates *katA*, encoding catalase, and *dspB*, encoding

Dispersin B, enabling both fight (using catalase) or flight (using Dispersin B) and overall promoting biofilm formation by both species.[27] There is evidence that *S. gordonii* and *F. nucleatum* respond to the presence of one another, since the total protein profiles of each species are distinct when grown in two- or three-species biofilms (also containing *P. gingivalis*) compared with monoculture biofilms.[28,29] However, the early changes in gene expression in these two important oral bacteria following cell-cell interactions have not yet been documented. Therefore, this study aimed to explore the impact of coaggregation between *S. gordonii* and *F. nucleatum* in human saliva on the gene expression in each partner. Understanding responses to coaggregation will provide important insights into how these species adapt as they interact with one another during the formation of oral biofilms.

MATERIALS AND METHODS

Saliva preparation

Ethical approval for the collection of saliva from healthy volunteers was obtained from the Newcastle University Research Ethics Committee (reference 1083). Parafilm-stimulated saliva was collected on ice from five healthy individuals who had not eaten for at least 2 h prior to collection. Immediately after collection, dithiothreitol (DTT) was added to a final concentration of 2.5 mM and stirred gently on ice for 10 min. Large particles were removed by centrifugation at 15,000 g for 30 min at 4°C. The supernatant was collected and 3 volumes of H_2O were added to 1 volume of saliva. The diluted saliva was sterilized by filtration through a 0.22 µm pore membrane. Saliva was aliquoted and stored at -20°C until use as a medium for coaggregation. Before use, saliva was thawed in a 37°C water bath and any precipitate that had formed was removed by centrifugation at 1,400 g for 10 min at 20°C.

Bacterial growth and coaggregation assays

S. gordonii DL1 was routinely grown statically at 37°C in THYE broth containing 30 g/L Bacto™ Todd Hewitt Broth (Becton Dickinson, Plymouth, UK), 5 g/L yeast extract (Melford Laboratories, Ipswich, UK). *Fusobacterium nucleatum* subsp. *nucleatum* ATCC 25586 was cultured at 37°C in Fastidious Anaerobe Broth (FAB) consisting of peptone mix 15.0 g/L, yeast extract 10.0 g/L, sodium thioglycollate 0.5 g/L, sodium chloride 2.5 g/L, sodium bicarbonate 0.4 g/L, L-cysteine HCl 0.5 g/L, haemin 0.005 g/L and vitamin K 0.0004 g/L (Lab M, Lancashire, UK), under anaerobic conditions (gas mix 90% N_2, 5% H_2 and 5% CO_2).

To assess coaggregation, *S. gordonii* DL1 and *F. nucleatum* ATCC 25586 were cultured separately for 18 h in THYE and FAB, respectively, and harvested by centrifugation at 3,800 *g* for 10 min in a swing-out rotor. Cells were washed three times with one volume of phosphate buffered saline (PBS, pH 7.3) and re-suspended in one volume of either coaggregation buffer (1 mM Tris-HCl pH 8.0, 0.1 mM $CaCl_2$, 0.1 mM $MgCl_2$, 150 mM NaCl, and 0.02% NaN_3) or saliva, prepared as above, to give an optical density of 1.0 at 600 nm (final concentration of approximately 10^9 CFU/mL). Coaggregation was induced by mixing 150 µL of each culture in a glass tube, mixing by vortex for 10 sec and gently rocking until coaggregation was visible. The formation of macroscopic coaggregates was assessed by the visual scoring system.[25] Three biological replicates were performed for all conditions.

Confocal scanning laser microscopy (CSLM) imaging of coaggregation

For CSLM imaging of coaggregation, *S. gordonii* DL1 and *F. nucleatum* 25586 were cultured in THYE and FAB as above, harvested and washed three times in coaggregation buffer. Cultures were adjusted to $OD_{600\,nm}$=1.0. To visualize *S. gordonii* cells, an aliquot of 500 µl of cells

was added to 5 µl PicoGreen dye (Life technologies Ltd, Paisley, UK). For visualizing *F. nucleatum*, propidium iodide (Sigma-Aldrich, Inc), was added to a concentration of 1.5 mM in 500 µl of bacterial cell suspension. Samples were incubated in darkness at 37°C for 30 min. Fluorescently stained bacteria were washed twice with coaggregation buffer and resuspended in 500 µl coaggregation buffer. To induce coaggregation in dual-species cultures, 500 µl of each species were mixed by vortex for 10 sec and gently rocked until coaggregation was visible.

Rubber O rings of 0.2 mm diameter (W&H Ltd, Bürmoos, Austria) were fixed to glass microscope slides using sticky wax or superglue. In order to keep the coaggregation stable during imaging, 0.25 volumes of agarose (1.25% wt/vol) were added to the sample. Cells were placed in the middle of the rubber ring and a coverslip (22 x 22 mm) was added. Coaggregation samples were visualized using a Leica SP2 CLSM microscope (3D) (Leica, Microsystems, Heidelberg, Germany) using excitation (Ex) at 530 nm and emission (Em) at 630 nm for propidium iodide and Ex/Em = 485 nm /530 nm for PicoGreen.

Electron microscopy

For high resolution imaging of coaggregation by transmission electron microscopy (TEM), coaggregation was induced as described above. Samples were placed into 2% (v/v) glutaraldehyde and stored at 4°C for up to 48 h. Samples were dehydrated through a series of ethanol washes, embedded in epoxy resin and sectioned at Electron Microscopy Research Services, Newcastle University. Sections were analyzed in a Philips CM100 transmission electron microscope. For serial block face sectioning-scanning electron microscopy (SBF-SEM), coaggregated cells were fixed in 2% glutaraldehyde for 24 h at 4°C, rinsed twice in PBS and then dehydrated through a series of ethanol washes: once each in 25%, 50%, 75%, and two times in 100% ethanol for 30 min. The structure of coaggregates was visualized using a Zeiss Sigma Field Emission Gun Scanning

Electron Microscope (FEGSEM) incorporating Gatan 3view. Approximately 100 serial 70 nm sections were analysed. *S. gordonii* and *A. oris* cells were manually identified and color-coded, facilitated by AMIRA 3D software (Thermo Fisher).

Extraction of RNA from coaggregates and monocultures

To assess gene regulation responses to coaggregation, *S. gordonii* and *F. nucleatum* were cultured for 18 h at 37°C in BHYG containing (per L): Brain Heart Infusion 37 g, Yeast extract 5 g and sodium glutamate 2.5 g. Cells were subcultured into fresh medium and grown to mid-exponential phase (OD_{600} = 0.4-0.6). Cells were harvested at 3,800 *g* in a swing out rotor at 20°C for 10 min and adjusted to OD_{600} = 1.0 +/- 0.2. Five mL of each culture was harvested at 3,800 *g*, 20°C for 5 min and resuspended in 0.5 ml human saliva. Samples were divided into two equal portions and one of each was used for monoculture controls, while the other portion of each cell type were combined and vortex mixed for 10 sec to induce coaggregation. All samples were made up to 5 mL by the addition of saliva and incubated at 37°C for 30 min. Five mL of RNA*later* (Invitrogen) was added, and the tubes were vortexed for 5 sec and incubated at 20°C for 5 min. Following incubation, cells were harvested at 3,000 *g* for 15 min at 20 °C, the supernatant was discarded, and the pellets were frozen at -80°C for RNA extraction within 7 days. Three biological replicates were performed for all conditions.

To disrupt cells for RNA extraction, samples were thawed at 20°C and resuspended in 100 µl spheroplasting buffer containing 0.1 mg/mL spectinomycin.[30] Mutanolysin was added to 500 U/mL and cells were incubated at 37°C for 5 min. Total RNA was extracted using the Ambion RiboPure Bacteria RNA Purification kit (Life Technologies) according to the manufacturer's instructions. RNA concentrations were determined using a NanoDrop ND-1000 Spectrophotometer (Thermo Scientific). To ensure that RNA had not degraded during extraction,

an aliquot of each sample was analyzed by gel electrophoresis. Additional quality control using the Bioanalyzer (Agilent Technologies, Santa Clara, CA, USA) was performed upon receipt of samples by BGI Tech Solutions (Hong Kong).

Library construction and whole-transcriptome sequencing.

Following an initial rRNA depletion, first strand cDNA synthesis was performed using random hexamer primers. The second-strand cDNA was synthesized using buffer, deoxynucleotides, RNase H and DNA polymerase I. Short fragments were purified, ends repaired and poly(A) tails added, prior to connecting sequencing adapters. Second strand cDNA was digested with uracil N-glycosylase and the product was purified before PCR amplification. Finally, the library was sequenced on the Illumina HiSeq^{TM} 2000 platform to obtain paired end reads (100 bp) through the established and internationally recognized sequencing provider BGI, Hong Kong.

Preprocessing raw sequence data

Raw reads were quality examined by FastQC (Babraham Bioinformatics, UK). To improve the quality of reads and remove adapter sequences, reads with quality score less than 20 were filtered with Trimmomatic-0.36,[31] which left only the high-quality reads for the downstream assembly. The pre-processed reads were again examined with FastQC. All sequence reads were deposited at the NCBI Sequence Read Archive (https://ncbi.nlm.nih.gov/sra/) under Accession number SRP148871.

Mapping reads to the reference genome, abundance estimation, and data normalization

First raw reads for monoculture samples were mapped to the *S. gordonii* (NC_009785.1) and *F. nucleatum* (NC_003454.1, supplementary data1). For coaggregate samples, the

preprocessed reads were aligned in two rounds independently to the above two reference genomes and designated as SgFn_Fn (reads of mixed culture mapped to *F. nucleatum*) and SgFn_Sg (reads of mixed culture mapped to *S. gordonii*). Alignment for all reads was performed using TopHat v2,[32] a splice junction mapper built upon the short read aligner Bowtie with default parameters. Mapping statistics were verified using SAMtools[33] flagstat. Read counts were collected with HTSeq version-0.6.1p1[34] with settings stranded=yes, mode=union and type=gene using corresponding GFF files obtained from NCBI. Normalization was performed using the Trimmed Mean of *M*-values.[35] The fold changes after normalization and $\log_2$ transformations for each comparison produced by in house scripts (Figure 4) were visualized by boxplots.

Pairwise differential expression analysis between mixed cultures (SgFn) and monoculture control (Sg, Fn) conditions were performed using the R package DESeq2 available under Bioconductor (www.bioconductor.org). Differential Expression was determined using the DESeq2 version 3.6.[36] This was done using the sequence of commands: newCountDataSet, estimateSizeFactors, estimateDispersions, and nbinomTest. For the estimateDispersions function the settings used are method = "per-condition", sharingMode = "maximum", fitType = "parametric". The differentially expressed genes were considered to be significant at $P_{adj} < 0.05$. A volcano plot exploring all differentially expressed genes from mixed and monoculture comparisons displaying the relation between $\log_2$ (fold change) and statistical significance (P_{adj}) values was generated using in house R scripts. Gene networks corresponding to the screened differentially expressed genes were retrieved from Search Tool for the Retrieval of Interacting Genes (STRING) database v10.5.[37] To highlight connected clusters of nodes, kmeans clustering was applied as described in figure legends.

Quantitative reverse transcriptase PCR (RT-qPCR)

Quantitative reverse transcriptase PCR was carried out using two steps for reverse transcription and PCR. The reverse transcription step was performed using the QuantiTect Reverse Transcription Kit (Qiagen, Valencia, CA). RNA samples extracted from *S. gordonii* and *F. nucleatum* cells were converted into cDNA according to manufacturer's instructions, with the modification that random hexamers (Bioline, Taunton, MA, USA) were used in place of the QuantiTect oligo-dT primers.[30] The cDNA samples were stored at -20°C until analysis by real-time PCR. Primers for RT-qPCR analysis are described in Table 1.

All RT-qPCR was performed using SYBR Green dye from the SensiMix SYBR No-ROX kit (Bioline). Each reaction contained 25 µL consisting of 0–15 ng template cDNA, forward/reverse primers each at 2 µM, 12.5 µL Power SyBr Green PCR mix and sterile deionized water. Standard curves consisting of serial ten-fold dilutions of *S. gordonii* DL1 or *F. nucleatum* 25586 chromosomal DNA, no template control and 'no RT' negative controls were included on each plate. Reactions were carried out using a DNA Engine Opticon 2 (BioRad, Watford, UK) as follows: 1. 95°C for 5 min; 2. 95°C for 10 s; 3. 60°C for 30 s; 4. plate read; 5. repeat from step 2 a further 39 times; 6. melting curve from 55-90°C, read every 1°C, hold for 5 sec. As a reference, the 16S rRNA gene of S. *gordonii* or *F. nucleatum* was measured and used to normalize the data. To assess the specificity of the reactions, melt curve analysis were performed on all samples and selected products were also assessed by agarose gel electrophoresis. Three biological replicates were performed for all RT-qPCR reactions.

RESULTS AND DISCUSSION

Coaggregation between *S. gordonii* and *F. nucleatum*

Initially, coaggregation between *S. gordonii* DL1 and *F. nucleatum* 25586 was assessed using the well-established visual scoring system.[25] Macroscopic aggregates were observed after mixing equal concentrations of each species in either coaggregation buffer or human saliva. These were scored '4+' in the visual assay, indicating strong coaggregation with a complete clearance of the background. Previously, it has been shown that *F. nucleatum* 25586 coaggregates with a variety of *Streptococcus* spp. in saliva diluted in growth medium.[38] In addition, *F. nucleatum* ATCC 23726 coaggregates strongly with *S. gordonii* DL1 in coaggregation buffer.[11] Therefore, it was not unexpected that *S. gordonii* DL1 and *F. nucleatum* 25586 would form strong coaggregates in buffer or saliva. Three-dimensional (3D) CSLM images showed *S. gordonii* and *F. nucleatum* cells interspersed throughout the coaggregate structure (Figure 1). There was evidence that the DNA-binding dye PicoGreen had transferred from *S. gordonii* to *F. nucleatum* since a yellow color was observed within the majority of red-stained *F. nucleatum* cells (Figure 1B). Monoculture cells of *F. nucleatum* stained with propidium iodide were entirely red (data not shown). Nevertheless, *F. nucleatum* cells were clearly seen to be in close proximity to *S. gordonii* cells. Whilst coaggregation between many different oral bacteria, and between bacteria from other environments, has been demonstrated,[6,39] relatively little is known about the spatial positioning of cells from different species within these coaggregates. Using fluorescence microscopy, it was shown that *S. gordonii* and *A. oris* cells were distributed quite evenly throughout coaggregates, and *S. gordonii* appeared to sense and respond to these interactions.[24] Our CSLM images of *S. gordonii* and *F. nucleatum* showed a similar distribution of cells, and also indicated that there was potential for the different species to sense one another.

To observe the interactions between *S. gordonii* and *F. nucleatum* more closely, coaggregates were sectioned and visualized by TEM (Figure 2). In these images, *S. gordonii* cells

were seen to be closely associated with *F. nucleatum*, consistent with an adhesin-receptor-driven interaction.[10-12] Finally, to observe these interactions at high resolution in three dimensions, coaggregates were analyzed using serial block face sectioning SEM (SBF-SEM). This method involves taking serial sections of a fixed depth (~70 nm was used here), through an embedded sample using an ultramicrotome contained within an SEM. The surface profile of each section is visualized by SEM, and the serial sections can be reconstructed into a three-dimensional image. Using image analysis tools, individual cells can be identified and color-coded (Figure 3). This method confirmed that *S. gordonii* and *F. nucleatum* cells interacted closely with one another throughout the three-dimensional coaggregate structure. These close interactions provide clear opportunities for cells of the different species to sense and respond to each other. To the best of our knowledge, SBF-SEM has not previously been used to visualize coaggregate structures. The high resolution of this technique and the ability to reconstruct 3D images offers great opportunities for the detailed characterization of different coaggregation interactions in future. This method may also be used to obtain structural information about biofilms.[40]

RNA extraction and RNA-Seq

To assess the gene regulation responses of *S. gordonii* and *F. nucleatum* to coaggregation, cells of each species were mixed in human saliva to induce coaggregation, incubated for 30 min, and RNA was extracted from coaggregates or monoculture controls. The RNA from each sample was shown to be free from excessive degradation by NanoDrop spectrophotometry, agarose gel electrophoresis and Agilent Bioanalyzer analysis (data not shown). In total, Illumina sequencing from the three mixed *S. gordonii* and *F. nucleatum* (SgFn) biological replicates yielded 107,348,188 raw reads and for monoculture samples *S. gordonii* and *F. nucleatum* yielded

109,436,214 and 108,200,956 reads, respectively (Supplementary Table 1). After removal of bases with quality score less than 20 in Trimmomatic-0.36 software, we retained ≥92% reads for all the samples. Subsequently, for monoculture 95% of aligned reads mapped to the *S. gordonii* reference genome and 98% of aligned reads mapped to the *F. nucleatum* reference genome. For mixed transcriptome samples, 30% of reads mapped to the *S. gordonii* genome and 60% of reads mapped to the *F. nucleatum* genome (Supplementary Table S1). Samples from mixed and monoculture samples showed a similar distribution of per-gene read counts per sample, as visualized by box plots (Figure 4), indicating that the distributions of data were quantitatively comparable between mixed coaggregate and monoculture samples and no batch effects.[41]

DESeq2 was used to compare coaggregate sample reads with two monoculture sample reads separately. A total of 119 *S. gordonii* genes (51 down-regulated and 68 up-regulated genes) and 16 *F. nucleatum* genes (2 down-regulated and 14 up-regulated) were found to be differentially expressed at a false discovery rate (P_{adj}) of 0.05. Volcano plots of genes that were differentially expressed in the two different comparisons illustrate distinct transcriptional profiles (Figure 5).

RT-qPCR validation of RNASeq data

To validate the gene regulation observed by RNASeq, a selection of genes was also monitored by RT-qPCR. Two up-regulated, two down-regulated and two non-regulated genes that were reasonably strongly expressed were selected from each species. The patterns of expression were very similar by RNA-Seq and RT-qPCR (Figure 6). In each case, there was a strong correlation between the two data sets (Pearson's correlation coefficients between 0.96-0.97, $P<0.01$). Therefore, overall the RT-qPCR analysis of gene expression closely matched that by RNA-Seq.

Gene regulation in *F. nucleatum*

Genes that were regulated in *F. nucleatum* in response to coaggregation with *S. gordonii* are listed in Table 2. Broadly, functions related to amino acid transport, calcium transport, catalytic activity/phosphorous metabolic process, lipid transport/metabolism and sialic acid catabolism were affected. The network of interacting genes was visualized using the STRING database (Figure 7). The most striking impact of coaggregation was on the expression of an eight-gene operon involved in sialic acid catabolism (FN1470-FN1477). All genes in this operon were significantly up-regulated between 2- and 5-fold in response to coaggregation. The genes in this operon encode the machinery for sialic acid uptake via a tripartite ATP-independent periplasmic transporter (SiaPQM) and catabolism by NanA/NanK/NanE to produce N-acetylglucosamine-6-phosphate.[42] In addition, there is a regulator (NanR) and two proteins of unknown function (FN1470 and FN1477). The N-acetylglucosamine-6-phosphate is a substrate for the enzymes NagA and NagB, which produce fructose-6-phosphate that can then enter glycolysis.[43] Genes encoding NagA/NagB were not differentially regulated in our RNA-Seq analysis.

It is not clear why sialic acid catabolism was affected by coaggregation. Free sialic acid is found in saliva within the healthy mouth at concentrations >40 mg/dl.[44] In addition, sialic acid is commonly present in host glycoproteins as a terminal residue on carbohydrate side chains.[45] Some strains of *S. gordonii*, including *S. gordonii* DL1, bind to host sialic acids on glycoproteins and catabolise free sialic acids in saliva.[46,47] However, these activities would likely lead to reductions in the available sialic acid, which would then repress sialic acid catabolism in *F. nucleatum*. It is possible that the regulation of sialic acid operon in coaggregates may have resulted from changes in the localised levels of free sugars such as glucose following coaggregation. Sugars are known

to modulate sialic acid catabolism genes in some bacteria. For example, in *Corynebacterium glutamicum*, sialic acid catabolism genes are down-regulated during growth in glucose or fructose due to regulation by NanR and possibly also by a global carbon catabolite repressor.[48] It is noteworthy that high sialic acid concentrations in saliva have been associated with periodontal disease.[44] *S. gordonii* is generally associated with periodontal health.[49] It is possible that *S. gordonii* indirectly reduces sialic acid in saliva by stimulating sialidase activity of neighbouring *F. nucleatum* cells.

In addition to the sialic acid utilisation operon, there were clear changes in gene expression of FN0796 and FN0798, which were upregulated 1.5- to 1.7-fold. These genes encode two key enzymes in gluconeogenesis: pyruvate phosphate dikinase (FN0796) that converts pyruvate to phosphoenol pyruvate, and fructose 1,6-bis-phosphatase (FN0798) that hydrolyzes fructose 1,6-bisphosphate to fructose 6-phosphate. Two genes were downregulated between 1.5- and 1.7-fold: one gene each in amino acid transport (FN0328) and calcium transport (FN1022). Genes FN1078, FN0938, and FN0940 were up-regulated between 1.5- and 1.8-fold, but their functions are unknown. It is possible that FN0938 and FN0940 are part of the same operon as FN0941, encoding gamma-glutamyltranspeptidase. This enzyme plays a role in synthesis and degradation of glutathione, a key protective agent against oxidative stress. In summary, a significant proportion of the gene regulation response of *F. nucleatum* to coaggregation appears to involve metabolic pathways that converge on fructose 6-phosphate.

Gene regulation in *S. gordonii*

Many more genes were regulated in *S. gordonii* following coaggregation than in *F. nucleatum*. In total, 119 genes were regulated in *S. gordonii* (Supplementary Table S2). Key

functions that were affected included carbohydrate metabolism (19 genes), amino acid metabolism (14 genes) and regulation of DNA metabolic process (4 genes; Table 3). By STRING database analysis, the major clusters of up-regulated genes were those related to DNA metabolic processes and three genes in tryptophan biosynthesis (Figure 8). The genes involved in DNA metabolism are predicted to encode a regulatory protein (RecX), an endonuclease (MutS2), a cell division protein (DivIB) and a DNA repair protein (RecN). In *Bacillus subtilis* MutS2 promotes homologous recombination and protects cells from DNA damage.[50] It is possible that the changes in DNA metabolism prime the *S. gordonii* cells for uptake and incorporation of foreign DNA following sensing of a different species.

The up-regulation of tryptophan biosynthesis genes, along with the cysteine biosynthesis gene *cysK*, was part of a larger global response involving regulation of amino acid metabolism. Genes in several amino acid metabolism pathways were down-regulated following coaggregation (Figure 9) including both histidine catabolism (*hut* genes) and histidine biosynthesis (*his* genes). It has recently been shown that coaggregation can be sensed through the action of the *S. gordonii* extracellular protein Challisin, which appears to release amino acids from neighbouring bacteria such as *Actinomyces oris*.[25] It is possible that Challisin also acts on *F. nucleatum*. Alternatively, there may be direct cross-feeding of amino acids between *S. gordonii* and *F. nucleatum*. It has already been shown that *F. nucleatum* can utilize ornithine that is released from *S. gordonii* in exchange for arginine,[23] and there may be other nutrient exchanges that have yet to be identified.

The largest set of co-ordinated changes in gene expression was related to carbohydrate uptake and metabolism. In particular, genes involved in lactose and galactose uptake and catabolism were down-regulated following coaggregation. The regulation of these operons has previously been studied in detail.[51] The expression of *lacG* or *lacA1* was strongly repressed by

glucose compared with lactose or galactose. Regulation of the operon is complex and appears to be mediated by a combination of LacR, the global catabolite repressor CcpA, and a transcriptional antitermination mechanism directed by LacT.[51] Here, there was a small decrease in *lacG* expression in coaggregates compared with monocultures. This may indicate an increase in the local availability of glucose in coaggregates, or possibly a decrease in lactose and/or galactose. Metabolic cross-feeding from carbohydrate metabolism is well-known to occur in mixed cultures of bacteria. For example, lactic acid released as a product of carbohydrate catabolism by *S. gordonii* is a key nutrient for *Veillonella parvula* or *Aggregatibacter actinomycetemcomitans*.[19,20] Alternatively, changes in carbohydrates may be driven by competition. In mixed-species cultures, *S. gordonii* uses galactose more efficiently than *S. mutans*, except in very low pH.[51] It is not clear whether *F. nucleatum* can utilise lactose or galactose more efficiently than *S. gordonii* and this will be the subject of future studies. The major changes in regulation of genes involved in carbohydrate metabolism are consistent with a previously published proteomic analysis. In this case, increased levels of enzymes for glycolysis and the pentose phosphate pathway were detected in dual-species *S. gordonii*/*F. nucleatum* cultures compared with *S. gordonii* monocultures, consistent with higher energy availability in mixed cultures.[28]

CONCLUSIONS

Coaggregation followed by dual RNA-Seq provides a simple model to analyse early responses to interactions between taxonomically distinct bacterial cells. We predict that the gene regulation will be similar to that following incorporation into biofilms, since the structure of aggregates is similar in many ways to a biofilm. The advantage of using aggregated cultures rather than biofilms is that there is no need for scraping cells from a surface to recover RNA, which could

potentially lead to changes in RNA levels as a result of sample processing. In future, it will be important to extend these studies by monitoring gene expression over a prolonged time course, as has been reported for *S. gordonii* interacting with *Porphyromonas gingivalis*.[52] In addition, it will be important to determine whether there are similarities in gene regulation following interactions with a range of different bacteria. Conserved regulatory responses may elucidate key functions involved generically for adaptation to mixed-species environments. Such functions would be excellent candidate targets for new methods to control the formation of mixed-species biofilms such as dental plaque. Finally, it will be important to determine the mechanism of cell-cell sensing, and in particular whether it is mediated by an actively secreted factor or by the physical process of cell-cell contact. This could be tested by killing one partner species prior to coaggregation and monitoring gene regulation in the other. Interestingly, it has been shown that aggregation of bacteria by synthetic polymers designed to sequester quorum sensing signals activates quorum sensing-regulated genes, indicating that aggregation and quorum sensing may have similar impacts on gene regulation.[53] Elucidation of cell-cell sensing mechanisms between oral bacteria is critical for the development of novel strategies designed to control dental plaque by interfering with intermicrobial interactions.

ACKNOWLEDGEMENTS

We are very grateful to Dr Graham Stafford, Sheffield University, for helping us to interpret the gene regulation data. WKM was supported by a PhD studentship from the Ministry of Higher Education and Scientific Research (Iraq), and Centre for Oral Health Research (Newcastle University). NK was supported from EPSRC grants EP/J004111/2 & EP/N031962/1.

FIGURE LEGENDS

Figure 1. CSLM analysis of coaggregation between *S. gordonii* and *F. nucleatum*. *S. gordonii* cells were pre-labelled with PicoGreen and appeared green, whereas *F. nucleatum* cells were labelled with propidium iodide (red). A. Three-dimensional overview of coaggregates. B. An enlarged single slice through the coaggregate, showing close association between *S. gordonii* and *F. nucleatum*. Note that *F. nucleatum* cells appeared to have uptaken some of the DNA-binding PicoGreen dye since they appeared yellow in the centre of the cells.

Figure 2. High resolution analysis of interactions between *S. gordonii* and *F. nucleatum* cells using TEM. The right panel shows an enlargement of approximately the area highlighted by a box in the left panel. *S. gordonii* cells (*Sg*) could be distinguished from *F. nucleatum* (*Fn*) by their shape and thick cell walls. Individual *F. nucleatum* cells were often intimately associated with multiple *S. gordonii* cells (left panel).

Figure 3. High resolution 3D imaging of coaggregation between *S. gordonii* and *F. nucleatum* by SBF-SEM. Serial sections separated by 70 nm were taken through a coaggregate and each section was visualized by SEM. A. A single slice shown at low magnification and overlaid with false color of *S. gordonii* (green) and *F. nucleatum* (red), applied manually and assisted by edge-finding tools of AMIRA software. B. Enlargement of panel A and shown as a reconstruction from multiple slices to give a 3D image of coaggregation. C. Overview of the entire block shown in 3D. D. An alternative 3D view of the coaggregation, showing the interactions between false-colored *S. gordonii* (green) and *F. nucleatum* (red).

Figure 4. Distribution of normalized read counts. Counts were normalized by the Trimmed Mean of *M*-values approach. Median counts from each sample are shown as thick black lines surrounded by a box representing the interquartile range, with whiskers that extend to two standard deviations from the median. Outlying observations are shown as open circles. Data from three biological repeats of each sample (labelled 1-3) are shown.

Figure 5. Differentially expressed genes in coaggregates versus monocultures for *F. nucleatum* (A) and *S. gordonii* (B). The y-axis corresponds to the mean expression value of $\log_{10}$ (P_{adj})**,** and the x-axis displays the $\log_2$ (fold change) value. The green and red dots correspond to significantly up and down regulated genes, respectively ($P_{adj} < 0.05$)**.** The black dots represent the genes whose expression levels did not reach statistical significance ($P_{adj} > 0.05$).

Figure 6. Validation of RNA-Seq data for selected genes using RT-qPCR. The expression of six *S. gordonii* genes and six *F. nucleatum* genes in coaggregate cultures compared with monocultures was monitored by RT-qPCR, normalized against the 16S rRNA gene. Means and SDs from three independent samples from RNASeq (dark bars) and RT-qPCR (light bars) are shown. In all cases, similar levels of expression of each gene were identified by RNA-Seq and RT-qPCR.

Figure 7. Network of genes upregulated in response to coaggregation, visualized using the STRING database. Nodes were clustered by kmeans clustering into 7 groups, represented by circles of different colours. Interactions between nodes are depicted by coloured lines. Different colours represent evidence from different sources such as gene neighbourhood (green), gene co-

occurrence (dark blue), text mining (yellow), curated databases (cyan), experimentally determined (magenta), coexpression (black), protein homology (light blue) and gene fusions (red). Genes involved in sialic acid catabolism form the strongest cluster (red circles).

Figure 8. Genes that were up-regulated in *S. gordonii* in response to coaggregation, visualised by STRING database analysis. Genes were coloured based on kmeans clustering into 3 distinct groups. Genes involved in DNA maintenance form one cluster (green nodes), while three genes for tryptophan biosynthesis form a separate cluster (blue nodes). Edges were drawn based on different lines of evidence (see legend to Figure 7).

Figure 9. STRING database analysis of genes down-regulated in *S. gordonii* following coaggregation. Five different clusters from kmeans clustering are indicated by different colours of nodes. See legend to Figure 7 for an explanation of the edges. The major cluster (light brown/green nodes) is formed from lactose/galactose uptake and catabolism genes that are co-located on the chromosome.

REFERENCES

1. Bowen WH, Burne RA, Wu H, Koo H. Oral biofilms: Pathogens, matrix, and polymicrobial interactions in microenvironments. *Trends Microbiol.* 2018;26:229-242.
2. GBD 2016 Disease and Injury Incidence and Prevalence Collaborators. Global, regional, and national incidence, prevalence, and years lived with disability for 328 diseases and injuries for 195 countries, 1990-2016: a systematic analysis for the Global Burden of Disease Study 2016. *Lancet.* 2017;390:1211-1259.
3. Nobbs AH, Jenkinson HF, Jakubovics NS. Stick to your gums: mechanisms of oral microbial adherence. *J Dent Res.* 2011;90:1271-1278.
4. Zijnge V, van Leeuwen MB, Degener JE, et al. Oral biofilm architecture on natural teeth. *PLoS One.* 2010;5:e9321.
5. Mark Welch JL, Rossetti BJ, Rieken CW, Dewhirst FE, Borisy GG. Biogeography of a human oral microbiome at the micron scale. *Proc Natl Acad Sci U S A.* 2016;113:E791-800.
6. Katharios-Lanwermeyer S, Xi C, Jakubovics NS, Rickard AH. Mini-review: Microbial coaggregation: ubiquity and implications for biofilm development. *Biofouling.* 2014;30:1235-1251.
7. Jakubovics NS, Strömberg N, van Dolleweerd CJ, Kelly CG, Jenkinson HF. Differential binding specificities of oral streptococcal antigen I/II family adhesins for human or bacterial ligands. *Mol Microbiol.* 2005;55:1591-1605.
8. Back CR, Douglas SK, Emerson JE, Nobbs AH, Jenkinson HF. *Streptococcus gordonii* DL1 adhesin SspB V-region mediates coaggregation via receptor polysaccharide of *Actinomyces oris* T14V. *Mol Oral Microbiol.* 2015;30:411-424.
9. Edwards AM, Grossman TJ, Rudney JD. Association of a high-molecular weight arginine-binding protein of *Fusobacterium nucleatum* ATCC 10953 with adhesion to secretory immunoglobulin A and coaggregation with *Streptococcus cristatus*. *Oral Microbiol Immunol.* 2007;22:217-224.
10. Kaplan CW, Lux R, Haake SK, Shi W. The *Fusobacterium nucleatum* outer membrane protein RadD is an arginine-inhibitable adhesin required for inter-species adherence and the structured architecture of multispecies biofilm. *Mol Microbiol.* 2009;71:35-47.
11. Lima BP, Shi W, Lux R. Identification and characterization of a novel *Fusobacterium nucleatum* adhesin involved in physical interaction and biofilm formation with *Streptococcus gordonii*. *Microbiologyopen.* 2017;6.
12. Kaplan A, Kaplan CW, He X, McHardy I, Shi W, Lux R. Characterization of *aid1*, a novel gene involved in *Fusobacterium nucleatum* interspecies interactions. *Microb Ecol.* 2014;68:379-387.
13. Guo L, Shokeen B, He X, Shi W, Lux R. *Streptococcus mutans* SpaP binds to RadD of *Fusobacterium nucleatum* ssp. *polymorphum*. *Mol Oral Microbiol.* 2017;32:355-364.
14. Foster JS, Kolenbrander PE. Development of a multispecies oral bacterial community in a saliva-conditioned flow cell. *Appl Environ Microbiol.* 2004;70:4340-4348.
15. Guo L, He X, Shi W. Intercellular communications in multispecies oral microbial communities. *Front Microbiol.* 2014;5:328.
16. Jakubovics NS. Intermicrobial Interactions as a Driver for Community Composition and Stratification of Oral Biofilms. *J Mol Biol.* 2015;427:3662-3675.

17. Kolenbrander PE, Palmer RJ, Jr., Periasamy S, Jakubovics NS. Oral multispecies biofilm development and the key role of cell-cell distance. *Nat Rev Microbiol.* 2010;8:471-480.
18. Marsh PD, Zaura E. Dental biofilm: ecological interactions in health and disease. *J Clin Periodontol.* 2017;44 Suppl 18:S12-s22.
19. Egland PG, Palmer RJ, Jr., Kolenbrander PE. Interspecies communication in *Streptococcus gordonii-Veillonella atypica* biofilms: signaling in flow conditions requires juxtaposition. *Proc Natl Acad Sci U S A.* 2004;101:16917-16922.
20. Brown SA, Whiteley M. A novel exclusion mechanism for carbon resource partitioning in *Aggregatibacter actinomycetemcomitans*. *J Bacteriol.* 2007;189:6407-6414.
21. Ramsey MM, Rumbaugh KP, Whiteley M. Metabolite cross-feeding enhances virulence in a model polymicrobial infection. *PLoS Pathog.* 2011;7:e1002012.
22. Kuboniwa M, Houser JR, Hendrickson EL, et al. Metabolic crosstalk regulates *Porphyromonas gingivalis* colonization and virulence during oral polymicrobial infection. *Nat Microbiol.* 2017;2:1493-1499.
23. Sakanaka A, Kuboniwa M, Takeuchi H, Hashino E, Amano A. Arginine-ornithine antiporter ArcD controls arginine metabolism and interspecies biofilm development of *Streptococcus gordonii*. *J Biol Chem.* 2015;290:21185-21198.
24. Jakubovics NS, Gill SR, Iobst SE, Vickerman MM, Kolenbrander PE. Regulation of gene expression in a mixed-genus community: stabilized arginine biosynthesis in *Streptococcus gordonii* by coaggregation with *Actinomyces naeslundii*. *J Bacteriol.* 2008;190:3646-3657.
25. Mohammed WK, Krasnogor N, Jakubovics NS. *Streptococcus gordonii* Challisin protease is required for sensing cell--cell contact with Actinomyces oris. *FEMS Microbiol Ecol.* 2018;94:fiy043.
26. Ramsey MM, Whiteley M. Polymicrobial interactions stimulate resistance to host innate immunity through metabolite perception. *Proc Natl Acad Sci U S A.* 2009;106:1578-1583.
27. Stacy A, Everett J, Jorth P, Trivedi U, Rumbaugh KP, Whiteley M. Bacterial fight-and-flight responses enhance virulence in a polymicrobial infection. *Proc Natl Acad Sci U S A.* 2014;111:7819-7824.
28. Hendrickson EL, Wang T, Dickinson BC, et al. Proteomics of *Streptococcus gordonii* within a model developing oral microbial community. *BMC Microbiol.* 2012;12:211.
29. Hendrickson EL, Wang T, Beck DA, et al. Proteomics of *Fusobacterium nucleatum* within a model developing oral microbial community. *Microbiologyopen.* 2014;3:729-751.
30. Jakubovics NS, Robinson JC, Samarian DS, et al. Critical roles of arginine in growth and biofilm development by *Streptococcus gordonii*. *Mol Microbiol.* 2015;97:281-300.
31. Bolger AM, Lohse M, Usadel B. Trimmomatic: a flexible trimmer for Illumina sequence data. *Bioinformatics.* 2014;30:2114-2120.
32. Kim D, Pertea G, Trapnell C, Pimentel H, Kelley R, Salzberg SL. TopHat2: accurate alignment of transcriptomes in the presence of insertions, deletions and gene fusions. *Genome Biol.* 2013;14:R36.
33. Dige I, Nyengaard JR, Kilian M, Nyvad B. Application of stereological principles for quantification of bacteria in intact dental biofilms. *Oral Microbiol Immunol.* 2009;24:69-75.
34. Anders S, Pyl PT, Huber W. HTSeq--a Python framework to work with high-throughput sequencing data. *Bioinformatics.* 2015;31:166-169.
35. Robinson MD, Oshlack A. A scaling normalization method for differential expression analysis of RNA-seq data. *Genome Biol.* 2010;11:R25.

36. Love MI, Huber W, Anders S. Moderated estimation of fold change and dispersion for RNA-seq data with DESeq2. *Genome Biol.* 2014;15:550.
37. Szklarczyk D, Franceschini A, Wyder S, et al. STRING v10: protein-protein interaction networks, integrated over the tree of life. *Nucleic Acids Res.* 2015;43:D447-452.
38. Merritt J, Niu G, Okinaga T, Qi F. Autoaggregation response of *Fusobacterium nucleatum*. *Appl Environ Microbiol.* 2009;75:7725-7733.
39. Stevens MR, Luo TL, Vornhagen J, et al. Coaggregation occurs between microorganisms isolated from different environments. *FEMS Microbiol Ecol.* 2015;91.
40. Kizilyaprak C, Bittermann AG, Daraspe J, Humbel BM. FIB-SEM tomography in biology. *Methods Mol Biol.* 2014;1117:541-558.
41. Fei T, Zhang T, Shi W, Yu T. Mitigating the adverse impact of batch effects in sample pattern detection. *Bioinformatics.* 2018:bty117-bty117.
42. Stafford G, Roy S, Honma K, Sharma A. Sialic acid, periodontal pathogens and *Tannerella forsythia*: stick around and enjoy the feast! *Mol Oral Microbiol.* 2012;27:11-22.
43. Caing-Carlsson R, Goyal P, Sharma A, et al. Crystal structure of N-acetylmannosamine kinase from *Fusobacterium nucleatum*. *Acta Crystallogr Sect F Struct Biol Cryst Commun.* 2017;73:356-362.
44. Rathod SR, Khan F, Kolte AP, Gupta M. Estimation of salivary and serum total sialic acid levels in periodontal health and disease. *J Clin Diagn Res.* 2014;8:ZC19.
45. Sonesson M, Ericson D, Kinnby B, Wickström C. Glycoprotein 340 and sialic acid in minor-gland and whole saliva of children, adolescents, and adults. *Eur J Oral Sci.* 2011;119:435-440.
46. Byers HL, Homer KA, Beighton D. Utilization of sialic acid by viridans streptococci. *J Dent Res.* 1996;75:1564-1571.
47. Wong A, Grau MA, Singh AK, Woodiga SA, King SJ. Role of neuraminidase-producing bacteria in exposing cryptic carbohydrate receptors for *Streptococcus gordonii* adherence. *Infect Immun.* 2018;86:e00068-18.
48. Uhde A, Brühl N, Goldbeck O, et al. Transcription of sialic acid catabolism genes in *Corynebacterium glutamicum* is subject to catabolite repression and control by the transcriptional repressor NanR. *J Bacteriol.* 2016;198:2204-2218.
49. Ge X, Rodriguez R, Trinh M, Gunsolley J, Xu P. Oral microbiome of deep and shallow dental pockets in chronic periodontitis. *PLoS One.* 2013;8:e65520.
50. Burby PE, Simmons LA. MutS2 promotes homologous recombination in *Bacillus subtilis*. *J Bacteriol.* 2017;199:e00682-00616.
51. Zeng L, Martino NC, Burne RA. Two gene clusters coordinate galactose and lactose metabolism in *Streptococcus gordonii*. *Appl Environ Microbiol.* 2012;78:5597-5605.
52. Hendrickson EL, Beck DA, Miller DP, et al. Insights into dynamic polymicrobial synergy revealed by time-coursed rna-seq. *Front Microbiol.* 2017;8:261.
53. Lui LT, Xue X, Sui C, et al. Bacteria clustering by polymers induces the expression of quorum-sensing-controlled phenotypes. *Nat Chem.* 2013;5:1058.

Table 1. Primers used for RT-qPCR

Target gene[a]	Gene description	Product length (bp)	Primer Sequence (5'-3')	
SGO_RS07445	galactose-6-phosphate isomerase	105	F	GTATGGTTGCAGCGGAAGTT
			R	GGCCTTCACCAACGATTTCA
SGO_RS07440	galactose-6-phosphate isomerase subunit LacB	116	F	CTAGCGGTCAGGCTGATCTT
			R	AGCTGAAGTCATATCACGTACCA
SGO_RS06265	30S ribosomal protein S21	133	F	ACTTCGCGGTAACGTGATTG
			R	CAAGTTTGCCGCATCCAGAA
SGO_RS09425	DUF1033 domain-containing protein	143	F	CGCAGTGATTTGATGACTGTCT
			R	TAACCCGGACGGTATTTGCT
SGO_RS00525	4-alpha-glucanotransferase	109	F	CTGTTCCTCATGCAATGCTC
			R	GGCAAGTTCATTCTTGCTGA
SGO_RS05765	Thioredoxin	96	F	AACTGCTTGCTCTGACGAGA
			R	GCTTCCTGACCGACAGCTA
SGO 16S rRNA	*S. gordonii* 16S rRNA	138	F	AGACACGGCCCAGACTCCTAC
			R	TCACACCCGTTCTTCTCTTACAA
FN1472	N-acetylneuraminate-binding protein	108	F	GCAGCTGCAAACTTAGCGTA
			R	TTCTTGACCATCAACTGCAT
FN1473	N-acetylneuraminate transporter small subunit	119	F	TCTGGAATGTCTGGTTCAGC
			R	CAAGAGGCAGCTGTAAGTCC
FN0328	Na(+)-linked D-alanine glycine permease	115	F	AGGTGTTTCACAATTGACAGGA

			R	TCCAGTTCCAACTTGTGCTG
FN1022	calcium-transporting ATPase	114	F	TTCTTGACCATCAACTGCAT
			R	GCTTTCTTTAGTGCAGGAGCA
FN0084	acetaldehyde dehydrogenase	92	F	AATGTAGGAGGGTCACTTGGA
			R	GTTGAACTTCCTCCGACTGC
FN0369	ribosomal-protein-alanine acetyltransferase	92	F	TTGTTTCTAGTGCTTCTGAACAAA
			R	TGCTAAGGCAGGAACAACTG
FN 16S rRNA	*F. nucleatum* 16S rRNA	130	F	CGGGACTTAACCCAACATCT
			R	AGGAACCTTACCAGCGTTTG

[a] 'SGO' numbers indicate *S. gordonii* genes, whereas 'FN' numbers refer to *F. nucleatum* genes.

Table 2. Genes regulated in *F. nucleatum* following coaggregation with *S. gordonii*.

Locus ID	Predicted function (gene)	Fold change[a]	P_{adj}
Amino acid transport			
FN0328	Na^+-linked D-alanine glycine permease	-1.49	0.04
Ca^{2+} transport			
FN1022	Ca^{2+}-transporting ATPase	-1.45	0.01
Catalytic activity or phosphorous metabolic process			
FN0796	Pyruvate phosphate dikinase	1.50	0.04
FN0798	Fructose-1,6-bisphosphatase (*fbp*)	1.65	<0.01
FN0938	Hypothetical protein	1.64	<0.01
Lipid transport/metabolism			
FN0940	Hypothetical protein	1.75	<0.01
FN0941	γ-glutamyltranspeptidase	1.67	<0.01
Sialic acid catabolism			
FN1470	Hypothetical protein	3.10	<0.01
FN1471	LacI family transcriptional regulator (*nanR*)	3.34	<0.01
FN1472	N-acetylneuraminate binding protein (*siaP*)	5.05	<0.01
FN1473	Sialic acid TRAP transporter permease protein (*siaQM*)	3.53	<0.01
FN1474	N-acetylmannosamine kinase (*nanK*)	2.97	<0.01
FN1475	N-acetylneuraminate lyase (*nanA*)	2.27	<0.01
FN1476	N-acetylmannosamine-6-phosphate 2-epimerase (*nanE*)	1.80	<0.01
FN1477	Hypothetical protein	2.01	<0.01
Function unknown			
FN1078	Hypothetical protein	1.67	<0.01

[a]Fold change in coaggregates versus monocultures. Negative numbers indicate down-regulation.

Table 3. Key groups of genes regulated in *S. gordonii* following coaggregation with *F. nucleatum*.

Locus ID	Predicted function (gene)	Fold change[a]	P_{adj}
Carbohydrate metabolism			
SGO_RS00510 (SGO_0102)	sugar ABC transporter permease	-1.55	0.02
SGO_RS00630 (SGO_0127)	RpiR family transcriptional regulator	1.66	0.03
SGO_RS01385 (SGO_0281)	PTS diacetylchitobiose transporter subunit IIC	1.50	<0.01
SGO_RS04560 (SGO_0932)	Galactokinase (*galK*)	-1.40	0.01
SGO_RS05460 (SGO_1112)	Phosphofructokinase (*fruB*)	-1.65	0.01
SGO_RS05465 (SGO_1113)	PTS fructose transporter subunit IIC (*fruA*)	-1.54	0.02
SGO_RS07410 (SGO_1512)	6-phospho-beta-galactosidase (*lacG*)	-1.30	0.03
SGO_RS07415 (SGO_1513)	PTS lactose transporter subunit IIBC (*lacE*)	-1.42	0.03
SGO_RS07420 (SGO_1514)	PTS lactose transporter subunit IIA (*lacF*)	-1.60	0.02
SGO_RS07430 (SGO_1516)	tagatose-bisphosphate aldolase (*lacD-2*)	-1.65	<0.01
SGO_RS07435 (SGO_1517)	tagatose-6-phosphate kinase (*lacC-1*)	-2.25	<0.01
SGO_RS07440 (SGO_1518)	galactose-6-phosphate isomerase (*lacB-2*)	-2.44	<0.01
SGO_RS07445 (SGO_1519)	galactose-6-phosphate isomerase (*lacA-1*)	-2.94	<0.01
SGO_RS07470 (SGO_1524)	tagatose-6-phosphate kinase (lacC-2)	-1.59	<0.01
SGO_RS07475 (SGO_1525)	galactose-6-phosphate isomerase (*lacB-1*)	-1.59	<0.01
SGO_RS07480 (SGO_1526)	galactose-6-phosphate isomerase subunit (*lacA-2*)	-1.85	<0.01
SGO_RS07720 (SGO_1576)	PTS cellobiose transporter subunit IIC (*ptcC*)	-1.53	0.01
SGO_RS08235 (SGO_1679)	PTS mannose transporter subunit IIAB	-1.54	<0.01
SGO_RS08625 (SGO_1759)	6-phospho-beta-glucosidase	-1.58	0.02
Amino acid metabolism			
SGO_RS02985 (SGO_0606)	Cysteine synthase (*cysK*)	-1.71	<0.01
SGO_RS03230 (SGO_0656)	Trytophan synthetase beta subunit (*trpB-2*)	-1.35	0.04
SGO_RS03245 (SGO_0659)	anthranilate phosphor-ribosyl transferase (*trpD*)	1.55	0.02
SGO_RS03255 (SGO_0661)	N-(5'-phosphoribosyl anthranilate isomerase (*trpF*)	1.59	0.05
SGO_RS04445 (SGO_0906)	2-isopropylmalate synthase (*leuA*)	-1.57	<0.01
SGO_RS05865 (SGO_1194)	Phosphoribosylanthranilate isomerase	1.46	0.04

SGO_RS06080 (SGO_1238)	Branched chain amino acid aminotransferase (*ilvE*)	-1.59	<0.01
SGO_RS06880 (SGO_1403)	phosphoribosyl-AMP cyclohydrolase (*hisI*)	-1.55	<0.01
SGO_RS06900 (SGO_1407)	Imidazoleglycerol-phosphate dehydratase (*hisB*)	-1.63	0.05
SGO_RS06915 (SGO_1410)	ATP phosphoribosyl transferase regulatory subunit (*hisZ*)	-1.55	0.02
SGO_RS07685 (SGO_1569)	N-acetyl-glutamate semialdehyde dehydrogenase (*argC*)	1.63	0.05
SGO_RS08850 (SGO_1804)	Imidazolonepropionase (*hutI*)	-1.52	0.01
SGO_RS08855 (SGO_1805)	Urocanate hydratase (*hutU*)	-1.50	<0.01
SGO_RS08860 (SGO_1806)	Glutamate formiminotransferase (*ftcD*)	-1.59	<0.01
Regulation of DNA metabolic process			
SGO_RS03085 (SGO_0626)	Regulatory protein (*recX*)	3.61	<0.01
SGO_RS01280 (SGO_0260)	DNA mismatch binding protein (*mutS2*)	2.43	0.05
SGO_RS03440 (SGO_0698)	DNA repair protein (*recN*)	1.52	0.01
SGO_RS05995 (SGO_1221)	Inorganic polyphosphate/ATP-NAD kinase (*nadK*)	1.51	0.03

[a]Fold change in coaggregates versus monocultures. Negative numbers indicate down-regulation.

Figure 1

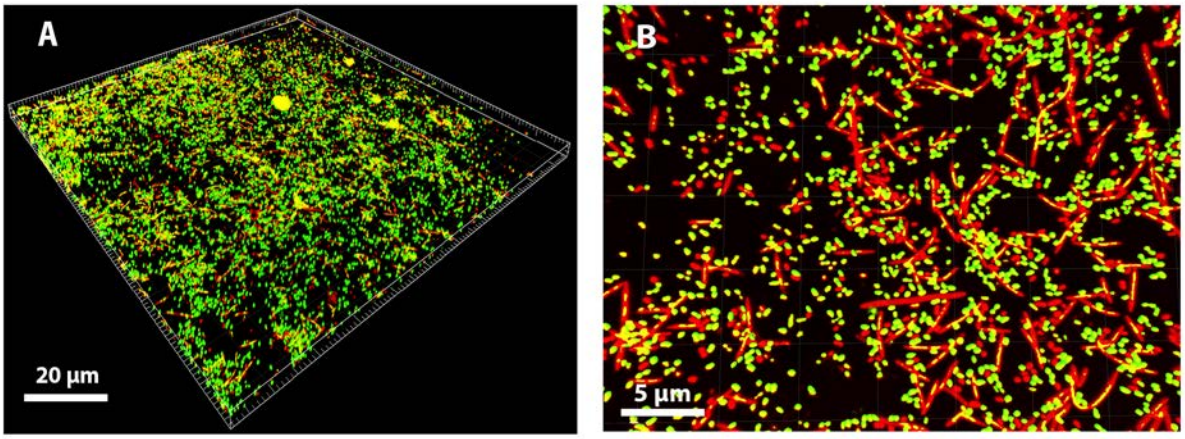

Figure 2

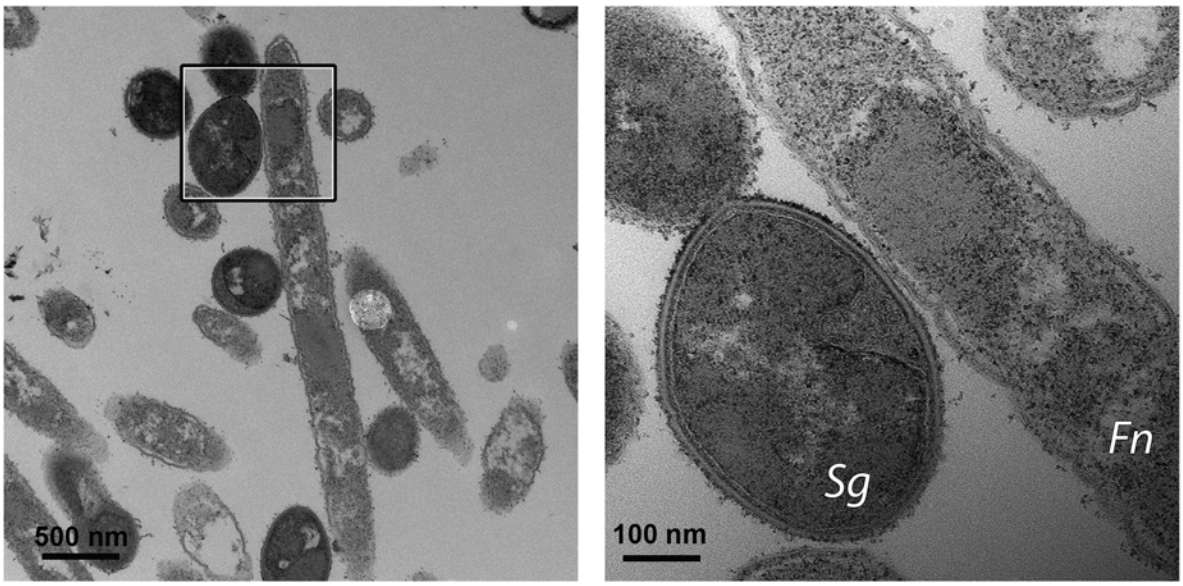

Figure 3

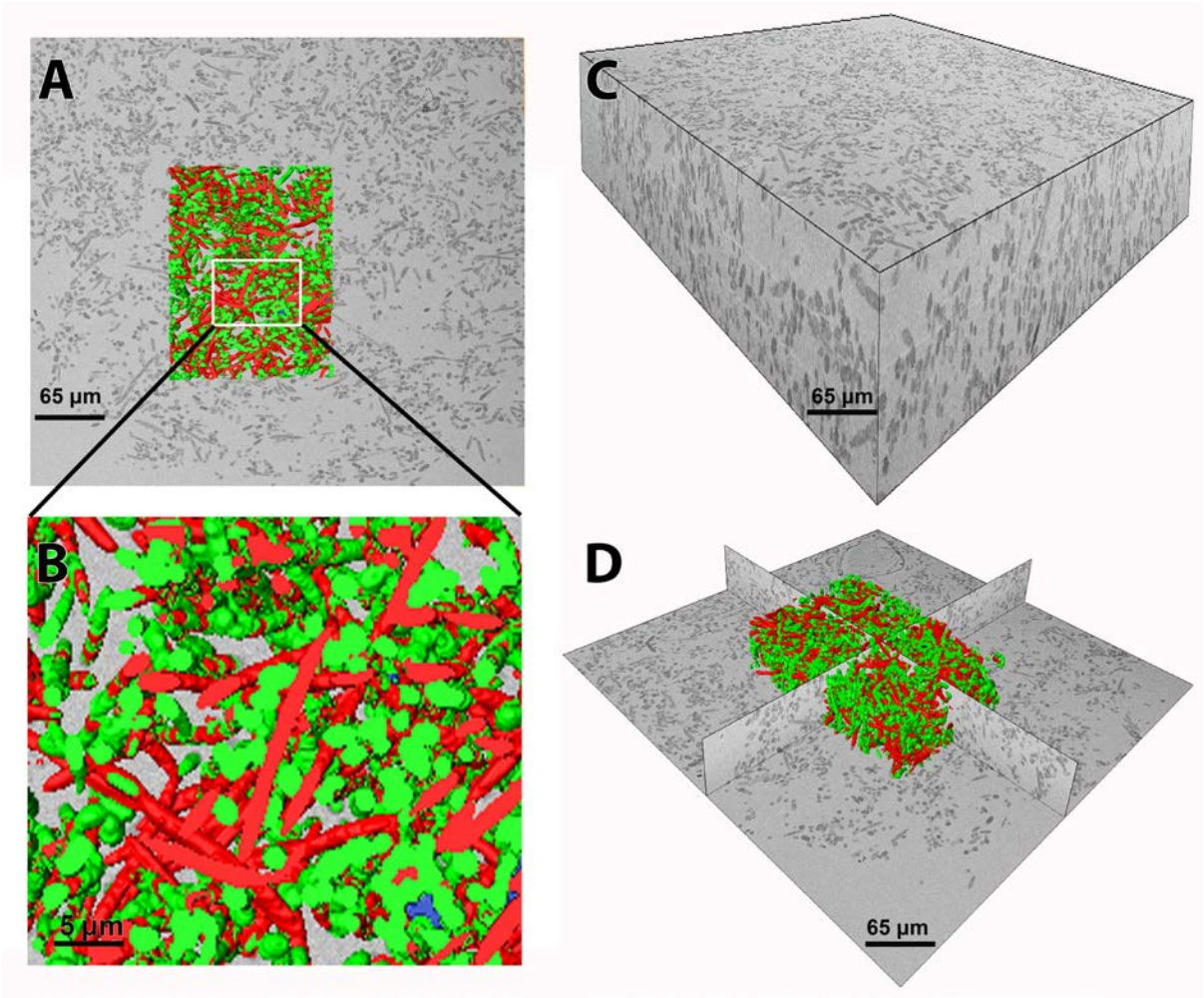

Figure 4

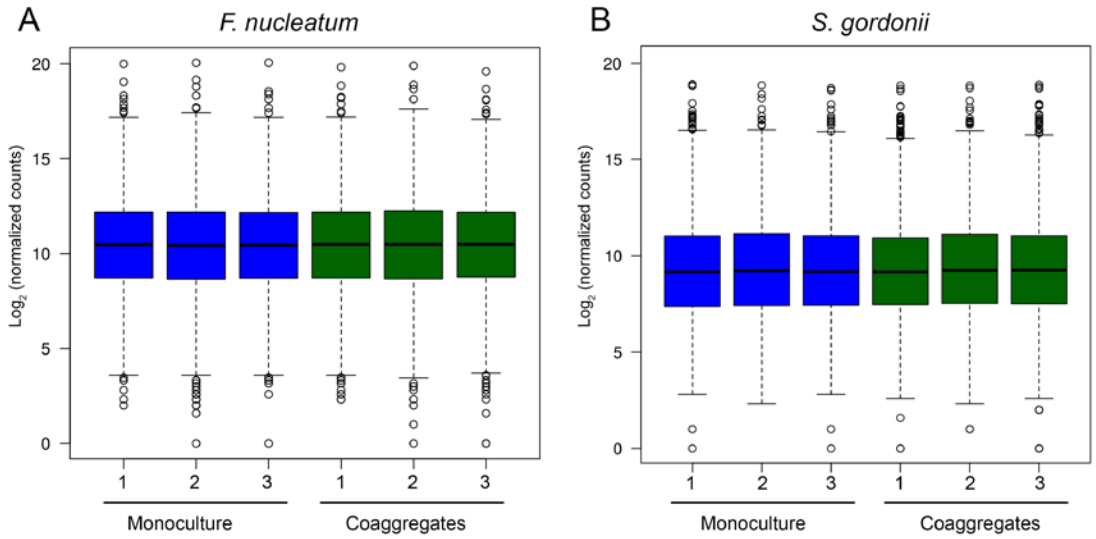
A
F. nucleatum
B
S. gordonii
Log2 (normalized counts)
20
15
10
5
0
1
2
3
Monoculture
Coaggregates

Figure 5

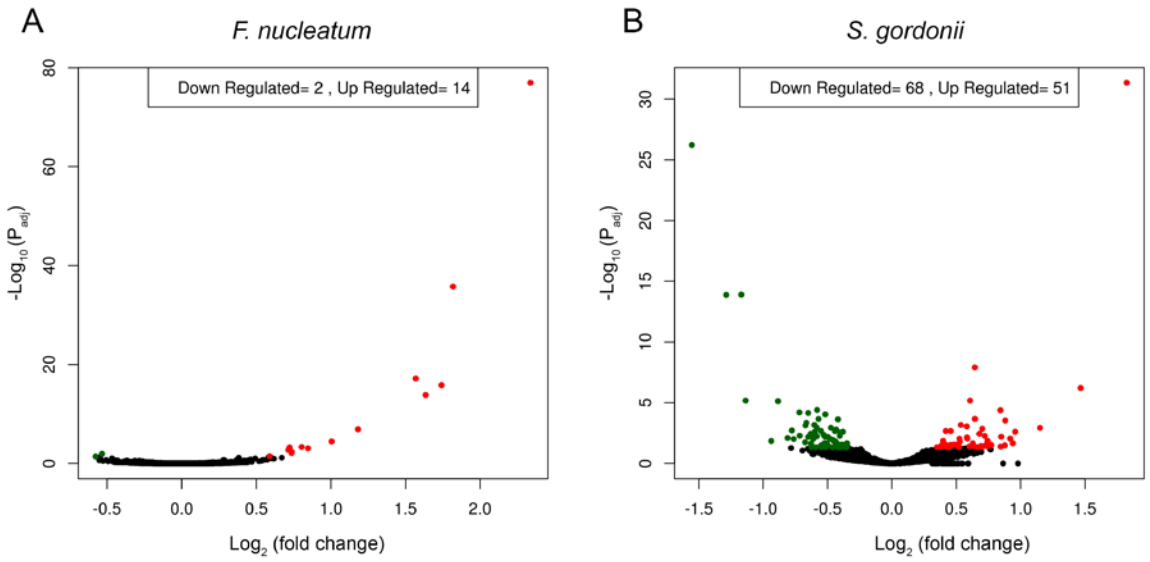
A
F. nucleatum
Down Regulated= 2 , Up Regulated= 14
-Log10 (Padj)
Log2 (fold change)
B
S. gordonii
Down Regulated= 68 , Up Regulated= 51
-Log10 (Padj)
Log2 (fold change)

Figure 6

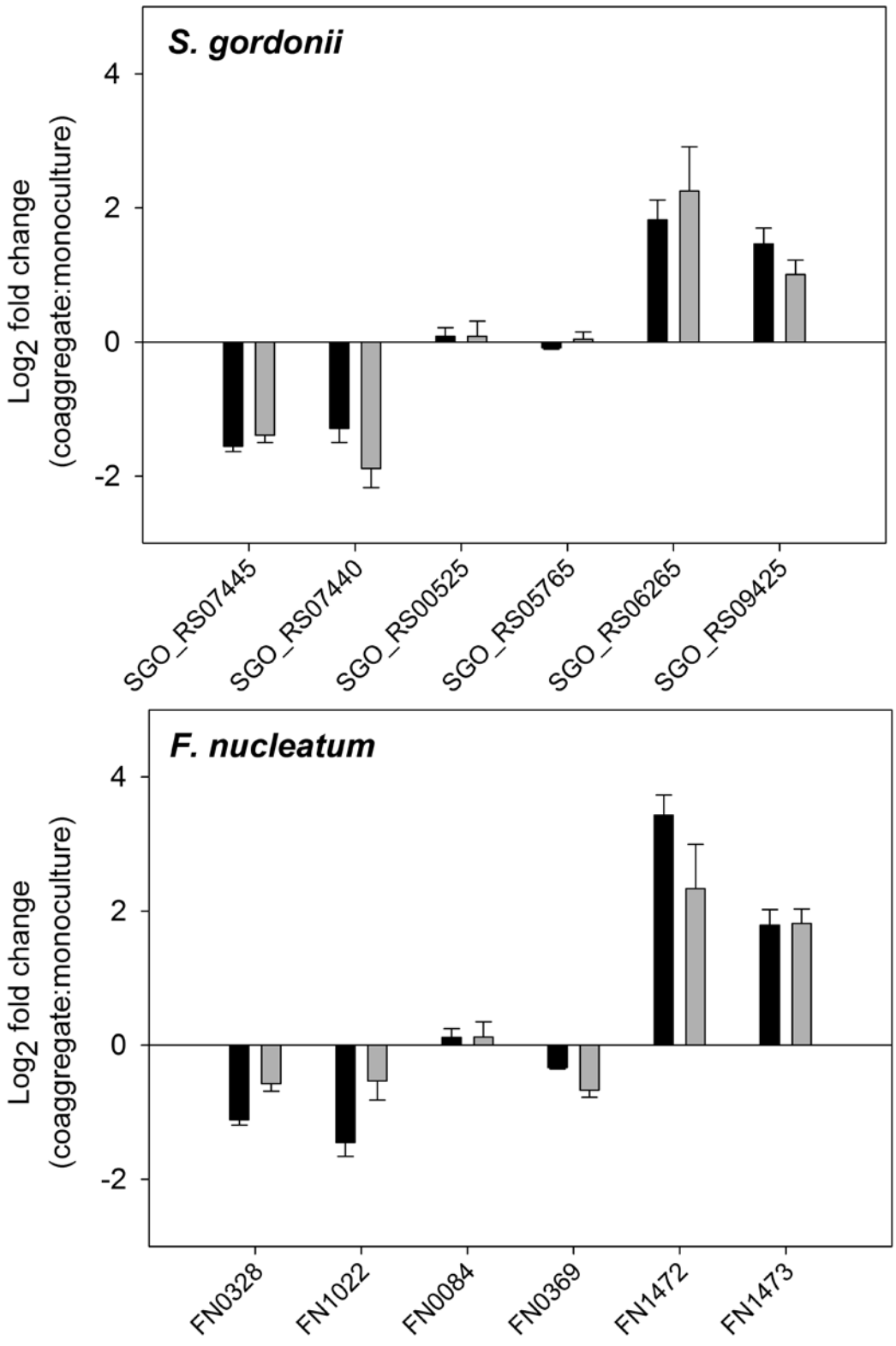
S. gordonii
Log2 fold change
(coaggregate:monoculture)
4
2
0
-2
SGO_RS07445
SGO_RS07440
SGO_RS00525
SGO_RS05765
SGO_RS06265
SGO_RS09425
F. nucleatum
Log2 fold change
(coaggregate:monoculture)
4
2
0
-2
FN0328
FN1022
FN0084
FN0369
FN1472
FN1473

Figure 7

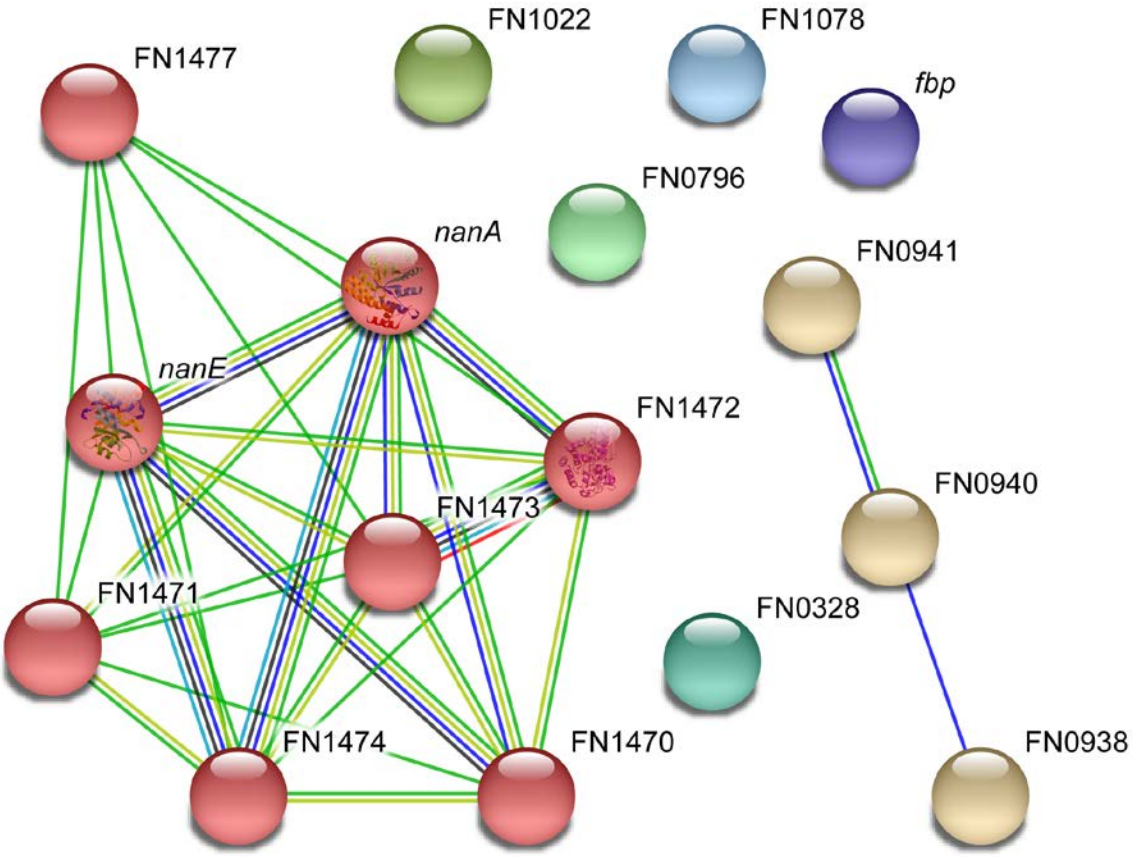
FN1022
FN1078
FN1477
fbp
FN0796
nanA
FN0941
nanE
FN1472
FN0940
FN1473
FN1471
FN0328
FN1474
FN1470
FN0938

Figure 8

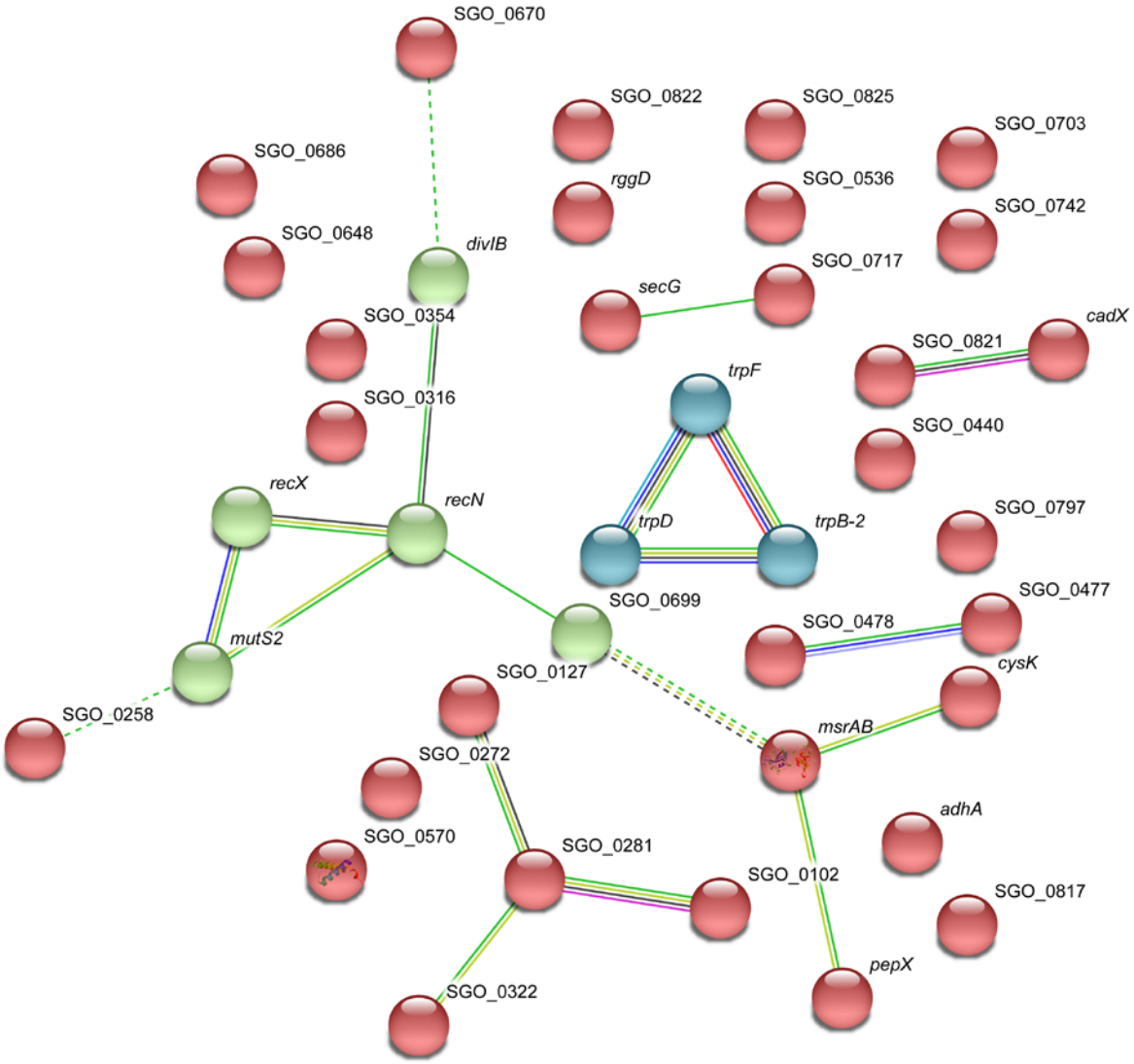
SGO_0670
SGO_0822
SGO_0825
SGO_0703
SGO_0686
rggD
SGO_0536
SGO_0742
SGO_0648
divIB
SGO_0717
secG
SGO_0354
cadX
SGO_0821
trpF
SGO_0316
SGO_0440
recX
recN
trpD
trpB-2
SGO_0797
SGO_0699
SGO_0477
SGO_0478
mutS2
cysK
SGO_0127
SGO_0258
msrAB
SGO_0272
adhA
SGO_0570
SGO_0281
SGO_0102
SGO_0817
pepX
SGO_0322

Figure 9

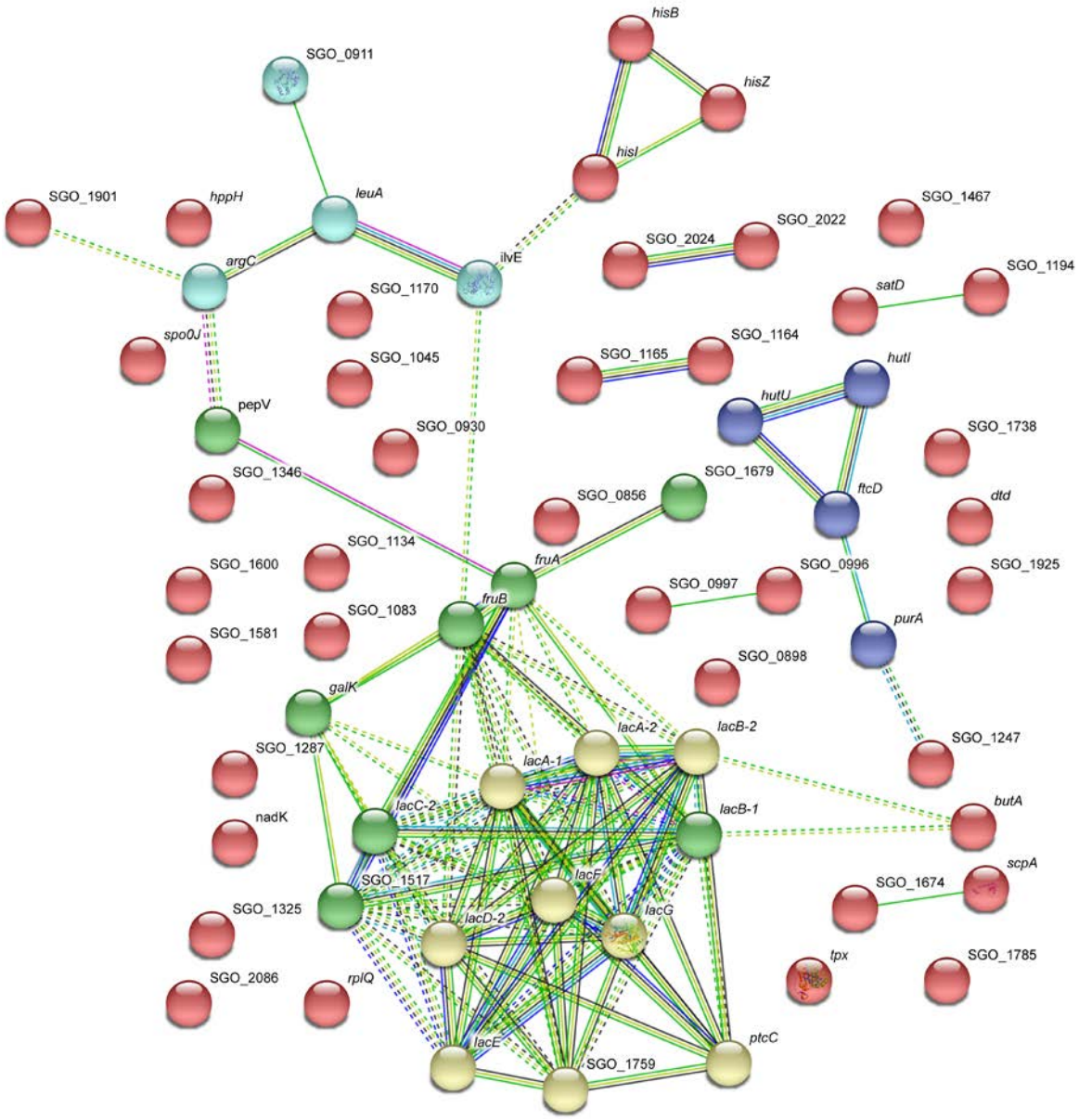
hisB
SGO_0911
hisZ
hisI
SGO_1901
hppH
leuA
SGO_1467
SGO_2022
SGO_2024
argC
ilvE
SGO_1194
satD
SGO_1170
spo0J
SGO_1164
SGO_1165
SGO_1045
hutI
hutU
pepV
SGO_0930
SGO_1738
SGO_1346
SGO_1679
SGO_0856
ftcD
dtd
SGO_1134
SGO_1600
fruA
SGO_0996
SGO_1925
SGO_0997
fruB
SGO_1083
purA
SGO_1581
SGO_0898
galK
lacA-2
lacB-2
SGO_1247
SGO_1287
lacA-1
lacC-2
lacB-1
butA
nadK
scpA
SGO_1674
SGO_1517
lacF
lacG
SGO_1325
lacD-2
tpx
SGO_1785
SGO_2086
rplQ
lacE
ptcC
SGO_1759